Journal of Solid State Chemistry 229 (2015) 287–295

Contents lists available at ScienceDirect

Journal of Solid State Chemistry

journal homepage: www.elsevier.com/locate/jssc

Structure and physical properties of RE_2AgGe_3 (RE=Ce, Pr, Nd) compounds

Sumanta Sarkar [a], Dundappa Mumbaraddi [a], Pramod Halappa [a], Deepti Kalsi [a], Sudhindra Rayaprol [b], Sebastian C. Peter [a,*]

[a] New Chemistry Unit, Jawaharlal Nehru Centre for Advanced Scientific Research, Jakkur, Bangalore 560064, India
[b] UGC-DAE Consortium for Scientific Research, Mumbai Centre, R-5 Shed, BARC Campus, Mumbai 400085, India

ARTICLE INFO

Article history:
Received 27 March 2015
Received in revised form
28 May 2015
Accepted 1 June 2015
Available online 17 June 2015

Keywords:
Intermetallics
Crystallography
Magnetism
Resistivity

ABSTRACT

We have synthesized the compounds RE_2AgGe_3 (*RE* =Ce, Pr, Nd) by arc melting. The crystal structure obtained from single crystal and powder X-ray diffraction suggests that these compounds crystallize in the α-$ThSi_2$ structure type. The magnetic susceptibility data of Ce_2AgGe_3 follows Curie–Weiss (CW) law above 25 K without any magnetic ordering down to 2 K. The effective magnetic moment (μ_{eff}) was calculated as 2.53 μ_B/Ce and negative Curie paramagnetic temperature (θ_p)= −2.4 K hint weak antiferromagnetic coupling among the adjacent spins. Pr_2AgGe_3 shows a complex magnetic behavior wherein the magnetic susceptibility at field cooled and zero field cooled modes bifurcates at 11.5 K with the latter undergoing a cusp like maxima, probably due to weak ferromagnetic interaction. The θ_p and μ_{eff} obtained are 4 K and 4.33 μ_B/Pr, respectively. Nd_2AgGe_3 undergoes multiple magnetic transitions. Temperature dependent resistivity data reveals that three compounds are metallic in nature.

1. Introduction

Rare-earth based compounds are one of the building blocks of material science due to their advanced application in the field of superconducting materials, magnetic materials, luminescent materials and hydrogen storage [1]. Recently, rare-earth based intermetallic compounds have been attracting much attention because of their versatile structural and physical properties such as intermediate valency [2], heavy fermion, Kondo behavior [3,4], spin glass behavior [5], superconductivity [6], structural phase transition [7], giant magnetoresistance [8], magnetocaloric effect [9] and zero thermal expansion [10]. These properties are associated with the presence of localized electronic 4*f* shell interaction with itinerant *s*, *p*, *d*-conduction electrons. Variable valences of cerium ($Ce^{3+/4+}$) can lead to many peculiar properties [11].

In this regard, it is interesting to briefly discuss about compounds crystallizing in the $ThSi_2$ structure type (both α and β-phases), particularly those with the general formula, RE_2TX_3 (RE=Ce, Pr, Nd; T=Transition metal, X=Si, In, Ge) owing to their fascinating structural and physical aspects. Here we give a brief overview on the compounds based on Ce, Nd and Pr. The examples are atom-disorder spin glass behavior was observed in Ce_2CuSi_3, Pr_2CuSi_3, Nd_2CuSi_3; Kondo lattice compound Ce_2NiGe_3 showed spin glass behavior; short range antiferromagnetic ordering was observed in Nd_2NiGe_3; annealed sample of Ce_2NiSi_3 showed antiferromagnetic transition at 4.2 K and additional anomaly at 2.5 K, Ce_2FeSi_3 and Ce_2PdSi_3 exhibit Kondo behavior and ferromagnetic ordering was observed below 16 K in Nd_2PdSi_3 [12–19], Kondo lattice reported in Ce_2IrSi_3 and Ce_2CoSi_3 [20,21]; weak spin glass behavior was observed in Nd_2PtSi_3 [22]. Ce_2RhSi_3 is antiferromagnetic below $T_N < 7$ K, ferromagnetic spiral magnetic ordering was observed at 4.2 K observed in a Nd_2RhSi_3 [21,23] and Ce_2CuGe_3 was reported as to show spin glass behavior [24]. All these compounds crystallize in the AlB_2 type structure (β-$ThSi_2$). Compounds crystallizing in the α-$ThSi_2$-type structure are $CeFe_{0.22}Si_{1.78}$ [25], $CeCu_{0.14}Ge_{1.71}$ [26], $CeTi_{0.23}Ge_{1.77}$ [27], $CeRh_{0.5}Ge_{1.5}$ [28], $PrNi_{0.25}Si_{1.75}$ [29], $PrNi_{0.07}Ge_{1.79}$ [30], $PrAg_{0.24}Ge_{1.76}$ [31], $PrCo_{0.3}Ge_{1.7}$ [32], $NdZn_{0.3}Si_{1.7}$ [33], $NdZn_{0.45}Si_{1.55}$ [34], $NdNi_{0.25}Si_{1.75}$ [35] and $NdNi_{0.25}Si_{1.75}$ [29]. Among the α-$ThSi_2$-type compounds, we have reported the spin glass behavior in $CeRh_{0.5}Ge_{1.5}$ [28]. The above mentioned works suggest that there may be other interesting compounds in the α-$ThSi_2$-type structure with interesting physical properties.

In comparison to the compounds with first row transition metals (e.g. Mn, Fe, Co, Ni, Cu), 4*d* and 5*d* block elements (e.g. Ru, Rh, Pd, Ag, Ir, Pt, Au) present an intriguing aspect to the overall physical properties of the compound because of the fact that 4*d*

* Corresponding author. Fax: +91 80 22082627.
E-mail address: sebastiancp@jncasr.ac.in (S.C. Peter).

http://dx.doi.org/10.1016/j.jssc.2015.06.003
0022-4596/

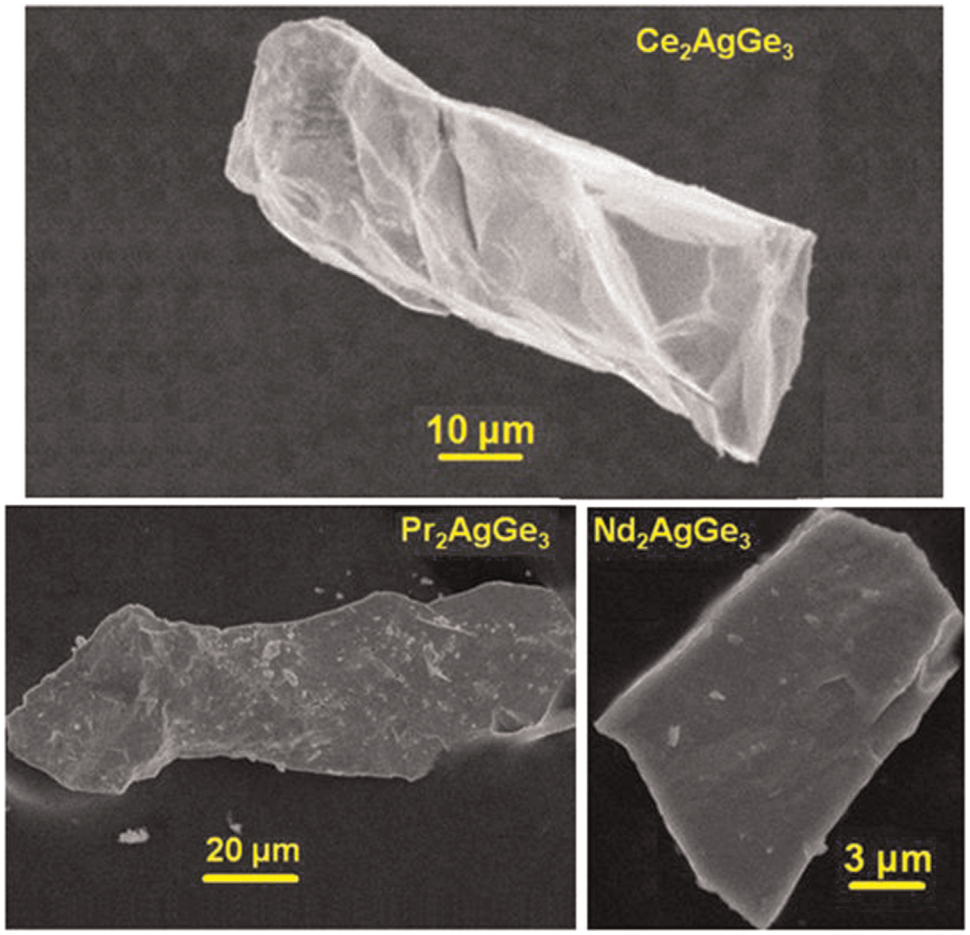

Fig. 1. FE SEM images of the single crystals of Ce_2AgGe_3, Nd_2AgGe_3 and Pr_2AgGe_3.

and 5*d* electrons can efficiently hybridize with the localized 4*f* orbitals belonging to lanthanide metals. This type of interaction dictates the conductivity and related properties of the itinerant electrons giving rise to interesting and very often anomalous properties. The other motivation of this work was our continuous search for new superstructures of the AlB_2 type structure similar to our recent studies on ordered compounds Eu_2AuSi_3, Eu_2AgGe_3, Eu_2AuGe_3, Yb_2AuSi_3 and Yb_2AuGe_3 [36–38], even though they were reported in the disordered structures earlier [29,39–41]. We also observed the lack of ordered structure as in $CeAu_xGe_{1-x}$ [42], $CeRh_xGe_{1-x}$ [28] and Nd_2NiGe_3 [43]; the first two led to the formation of the mixture of hexagonal and tetragonal crystal systems, but later one crystallize only with AlB_2 type. Understanding all these analyses, we have synthesized three Ag based compounds RE_2AgGe_3 (RE=Ce, Pr, Nd) by arc melting method. Our detailed powder and single crystal XRD measurements suggest that they are crystallizing in the α-$ThSi_2$ structure type. All three compounds found to be pure and further studied for their magnetic and transport properties in detail. All three compounds show diverse magnetic properties and are metallic in nature.

2. Experimental

2.1. Synthesis

The following metals were used as purchased without any further purification; Rare earth (Ce, Pr and Nd chunks, 99.99%, Alfa-Aesar), Ag (shots, 99.99%, Alfa-Aesar) and Ge (pieces, 99.999%, Alfa-Aesar). In a typical procedure, rare earth, silver and germanium metals were taken in an ideal 2:1:3 atomic ratios (total weight of reactant was ~200 mg) and repeatedly arc melted (flipping 5 times with 30 s arc passing) in an argon atmosphere to ensure homogeneity; hard globules were formed. Finally, the samples were crushed and made into powder for further characterization. All the samples are stable under normal atmospheric conditions for several months.

2.2. Elemental analysis

Semi quantitative microanalyses were performed on Ce_2AgGe_3, Pr_2AgGe_3 and Nd_2AgGe_3 single crystals using a Leica 220i electron microscope (SEM) equipped with Bruker 129 eV energy dispersive X-ray analyzer (EDS). Data were acquired with an accelerating voltage of 20 kV and 90 s accumulation time. The EDS analysis performed on cleaned surfaces of the single crystals percent showed the atomic composition for Ce_2AgGe_3 is 33.16(2) Ce, 20.90 (1) Ag and 45.94(1) Ge; for Pr_2AgGe_3 31.64(2), 19.17(1) and 49.19 (1); for Nd_2AgGe_3 33.62(3) Nd, 18.20(1) Ag, 48.18(1) Ge. The compositions obtained from EDS data are in good agreement with the results derived from the refinement of single crystal X-ray diffraction data. Field emission scanning electron microscopy (FE SEM) images of the representative single crystals are shown in Fig. 1.

2.3. Powder X-ray diffraction

The phase identity and purity of the samples were confirmed by powder XRD measurements carried out with on a Bruker D8 Discover diffractometer using Cu-Kα radiation (λ=1.5406 Å). All

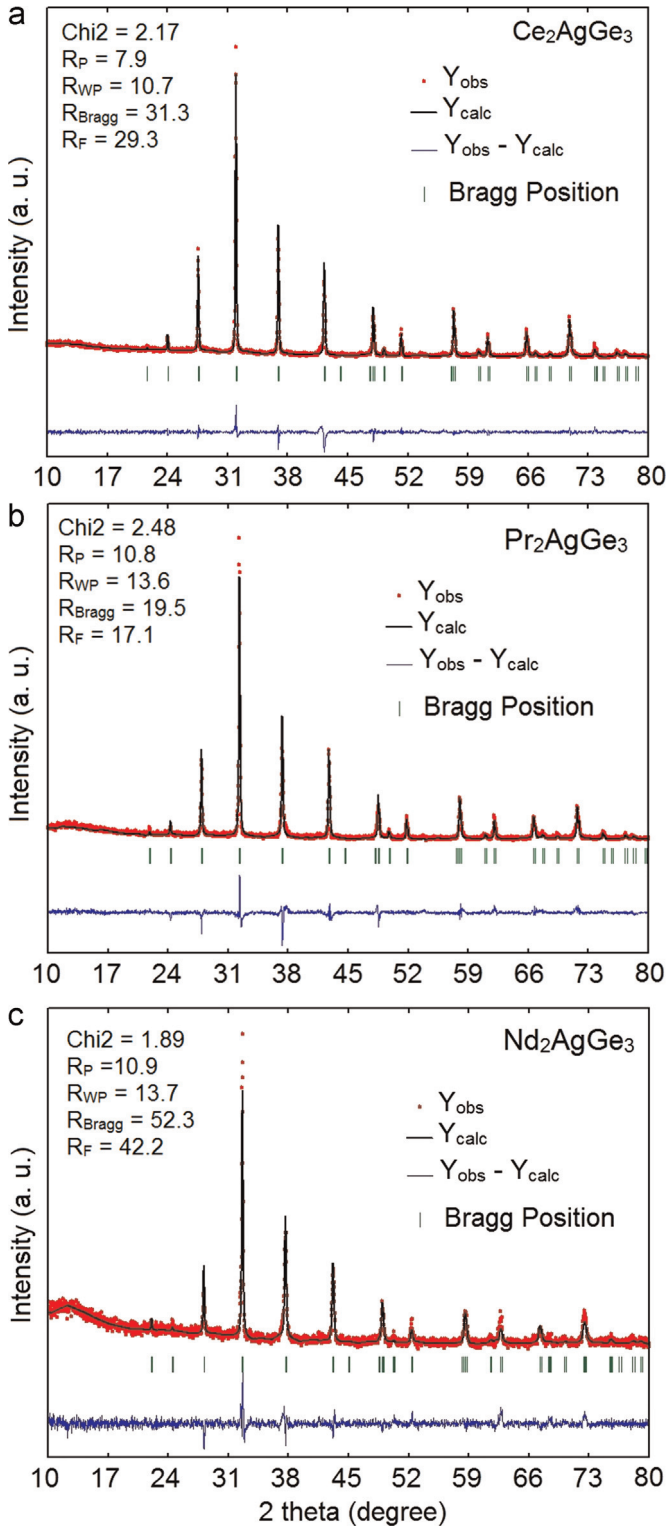

Fig. 2. Reitveld refinement of experimental powder XRD patterns of (a) Ce_2AgGe_3, (b) Pr_2AgGe_3 and (c) Nd_2AgGe_3 collected at 293 K using models obtained from the single crystal data refinement of each compound.

the samples were scanned for 1 h in the 2θ range of 10–90° with 0.02° step size at room temperature (293 K). Reitveld refinement was performed on all the three samples using the models obtained from the single crystal XRD data as shown in Fig. 2. The lattice parameters obtained from the Reitveld refinement for all the above compounds were comparable with the values obtained from the SCXRD data and have been summarized in Table S1.

2.4. Single-crystal X-ray diffraction

Selected single crystals of Ce_2AgGe_3, Pr_2AgGe_3 and Nd_2AgGe_3 were mounted on the tip of a glass fiber with glue. The single crystal data sets were collected on Bruker smart Apex-II CCD diffractometer equipped with Mo Kα radiation X-ray tube (λ=0.71073 Å) and a graphite monochromator with ω scan mode

Table 1
Crystal data and structure refinement for Ce_2AgGe_3, Pr_2AgGe_3 and Nd_2AgGe_3 at 293(2) K, and wavelength of Mo (0.71073 Å). Crystal system – tetragonal, space group – $I4_1/amd$, $Z=2$.

Empirical formula	$Ce_2Ag_{1.06}Ge_{2.94}$	$Pr_2Ag_{1.23}Ge_{2.77}$	$Nd_2Ag_{1.08}Ge_{2.92}$
Formula weight	608.13	615.69	617.08
Unit cell dimensions	$a=4.2754$ (3) Å	$a=4.2401$ (6) Å	$a=4.1886$ (6) Å
	$b=4.2754$ (3) Å	$b=4.2401$ (6) Å	$b=4.1886$ (6) Å
	$c=14.6855$ (16) Å	$c=14.611$ (3) Å	$c=14.557$ (3) Å
Volume	268.44 (4) $Å^3$	262.68 (8) $Å^3$	255.39 (7) $Å^3$
Density (calculated)	7.583 g/cm^3	7.747 g/cm^3	8.055 g/cm^3
Absorption coefficient	36.192 mm^{-1}	38.303 mm^{-1}	40.650 mm^{-1}
$F(000)$	524	527	531
Crystal size	$0.1\times0.08\times0.05$ mm^3	$0.16\times0.07\times0.04$ mm^3	$0.12\times0.09\times0.08$ mm^3
θ range for data collection	4.97–29.15°	5.01–27.21°	5.06–28.68°
Index ranges	$-5<=h<=5$,	$-4<=h<=5$,	$-5<=h<=4$,
	$-5<=k<=4$,	$-5<=k<=5$,	$-5<=k<=5$,
	$-20<=l<=15$	$-18<=l<=13$	$-8<=l<=19$
Reflections collected	604	530	983
Independent reflections	113 [$R_{int}=0.0675$]	98 [$R_{int}=0.0497$]	109 [$R_{int}=0.0186$]
Completeness to $\theta=27.21°$	98.3%	100%	100%
Refinement method	Full-matrix least-squares on F^2		
Data/restraints/parameters	113/0/9	98/0/9	109/0/9
Goodness-of-fit	1.162	1.441	1.256
Final R indices [$>2\sigma(I)$]	$R_{obs}=0.0553$,	$R_{obs}=0.0506$,	$R_{obs}=0.0474$,
	$wR_{obs}=0.1332$	$wR_{obs}=0.1128$	$wR_{obs}=0.1080$
R indices [all data]	$R_{all}=0.0594$,	$R_{all}=0.0557$,	$R_{all}=0.0481$,
	$wR_{all}=0.1364$	$wR_{all}=0.1165$	$wR_{all}=0.1086$
Extinction coefficient	0.0077 (3)	0.00259 (18)	0.00642 (19)
Largest diff. peak and hole	3.538 and −3.375 e $Å^{-3}$	2.330 and −3.219 e $Å^{-3}$	2.665 and −3.899 e $Å^{-3}$

$R=\Sigma||F_o|-|F_c||/\Sigma|F_o|$, $wR=\{\Sigma[w(|F_o|^2-|F_c|^2)^2]/\Sigma[w(|F_o|^4)]\}^{1/2}$ and calc $w=1/[\sigma^2(Fo^2)+(0.0481P)^2+54.6597P]$ where $P=(Fo^2+2Fc^2)/3$.

Table 2
Atomic coordinates ($\times10^4$) and equivalent isotropic displacement parameters ($Å^2\times10^3$) for Ce_2AgGe_3, $Pr_2AgGe_3$and Nd_2AgGe_3 at 293(2) K with estimated standard deviations in parentheses.

Label	Wyckoff site	x	y	z	Occupancy	U_{eq}*
Ce_2AgGe_3						
Ce	4*a*	0	7500	1250	1	5 (1)
M(Ag+Ge)	8*e*	0	2500	2918 (1)	0.27 (1)+0.73 (1)	20 (1)
Pr_2AgGe_3						
Pr	4*a*	0	7500	1250	1	19 (1)
M(Ag+Ge)	8*e*	0	2500	2919 (1)	0.31 (1)+0.69 (1)	39 (1)
Nd_2AgGe_3						
Nd	4*a*	0	7500	1250	1	11 (1)
M(Ag+Ge)	8*e*	0	2500	2918 (1)	0.27 (1)+0.73 (1)	31 (1)

* U_{eq} is defined as one third of the trace of the orthogonalized U_{ij} tensor.

Table 3
Anisotropic displacement parameters ($Å^2\times10^3$) for Ce_2AgGe_3, Pr_2AgGe_3 and Nd_2AgGe_3 at 293(2) K with estimated standard deviations in parentheses.

Label	U_{11}	U_{22}	U_{33}	U_{12}	U_{13}	U_{23}
Ce_2AgGe_3						
Ce	3 (1)	3 (1)	10 (1)	0	0	0
M(Ag+Ge)	16 (1)	23 (1)	21 (1)	0	0	0
Pr_2AgGe_3						
Pr	16 (1)	16 (1)	26 (1)	0	0	0
M(Ag+Ge)	34 (1)	37 (1)	45 (1)	0	0	0
Ce_2AgGe_3						
Nd	11 (1)	11 (1)	10 (1)	0	0	0
M(Ag+Ge)	28 (1)	38 (1)	28 (1)	0	0	0

The anisotropic displacement factor exponent takes the form: $-2\pi^2[h^2a^{*2}U_{11}+\ldots+2hka^*b^*U_{12}]$.

at 293 K. The crystal structures of Ce_2AgGe_3, Pr_2AgGe_3 and Nd_2AgGe_3 were successfully refined in the tetragonal $I4_1/amd$ space group by using SHELXS 97 [44] and refined by a full matrix least-squares method using SHELXL [45] with anisotropic atomic displacement parameters (ADP) for all the atoms. The atomic parameters of α-$ThSi_2$ were taken in which Si site is mixed with Ag and Ge atoms. The rare earth and mixed (M=Ag+Ge) sites are occupied at Wyckoff positions of 4*a* and 8*e*, respectively. Crystal structures were drawn using Diamond program [46]. Details of crystal data and structure refinement, atomic coordinates, equivalent isotropic displacement parameters and anisotropic displacement parameters for all three compounds are summarized in Tables 1–3. Further information on the structure refinements is available from: Fachinformationszentrum Karlsruhe, D-76344 Eggenstein-Leopoldshafen (Germany), by quoting the Registry no. CSD-429394, CSD-429394 and CSD-429394 for Ce_2AgGe_3, Pr_2AgGe_3 and Nd_2AgGe_3, respectively.

2.5. Magnetic measurements

Magnetic measurements were performed on single phase polycrystalline Ce_2AgGe_3, Pr_2AgGe_3 and Nd_2AgGe_3 samples using Quantum design superconducting quantum interference device (QD-SQUID) magnetic property measurement system (MPMS). Magnetic susceptibility of all the compounds were measured in zero field cooled (ZFC) and field cooled (FC) modes under different applied magnetic fields as a function of temperature. Field dependent magnetization measurements were also carried out at selected temperatures as a function of applied magnetic field.

2.6. Resistivity

The resistivity measurements were performed on the sintered (500 °C for 12 h in a evacuated quartz tube) pellets prepared in a rectangular die of size 8×2.5 mm^2 with thicknesses 0.44, 0.41 and 0.42 mm respectively for the samples Ce_2AgGe_3, Pr_2AgGe_3 and Nd_2AgGe_3 over the temperature range of 3–200 K using a four-probe dc technique. The compactness of the pellets was 53.7%, 54.2% and 51.5%, respectively. Four very thin copper wires with thickness of 50 μm were glued with the help of silver epoxy paste to the pellets. The measurements were conducted using a

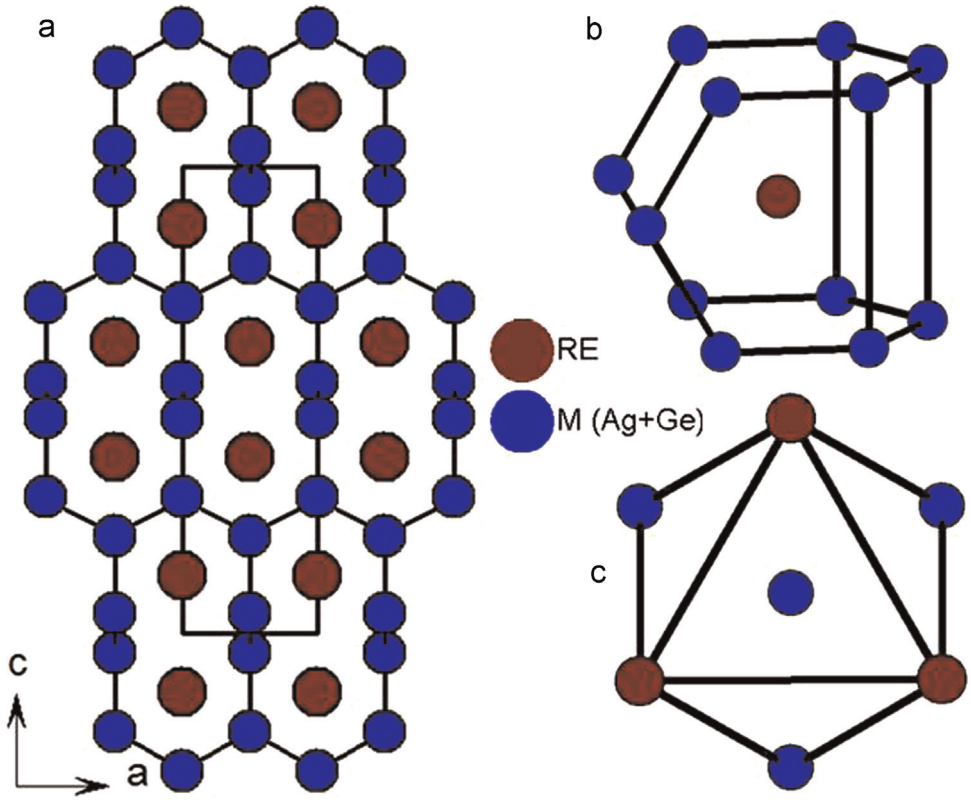

Fig. 3. (a) Crystal structures of RE_2AgGe_3 (b) coordination spheres of RE and (c) M (Ag+Ge) atoms in the crystal structure of RE_2AgGe_3 are presented.

Table 4
Selected bond lengths for Ce2AgGe3, Pr2AgGe3 and Nd2AgGe3 [Å] at 293(2) K with estimated standard deviations in parentheses.

Label	Distance	Label	Distance
Ce_2AgGe_3			
M–M	2.4446 (14) Å	M–M	2.4647 (7) Å
Ce-M	3.2508 (7) Å	Ce–M	3.2609 (3) Å
Pr_2AgGe_3			
M–M	2.429 (2) Å	M–M	2.4479 (12) Å
Pr–M	3.2311 (10) Å	Pr–M	3.2348 (6) Å
Nd_2AgGe_3			
M–M	2.4211 (16) Å	M–M	2.4228 (8) Å
Nd–M	3.1996 (5) Å	Nd–M	3.2069 (7) Å

Quantum Design Physical Property Measurement System (QD-PPMS) at an applying voltage of 95 mV and current of 0.1 mA.

3. Results and discussion

3.1. Crystal structure

The crystal structures of the compounds Ce_2AgGe_3, Pr_2AgGe_3 and Nd_2AgGe_3 are shown in Fig. 3. They crystallize in the α-$ThSi_2$ structure type having $I4_1/amd$ space group. The detailed crystal structure description can be available elsewhere [28]. The voids and channels of polyanionic network created by three-dimensional perpendicular [$AgGe_3$] layers were occupied by two rare earth atoms. The [$AgGe_3$] layers in the tetragonal crystal system stacked in AABB types and arranged perpendicular to each other. The weak interaction between the rare earth atoms is apparent from the bond distance of Ce–Ce (4.2754(3) Å), Pr–Pr (4.2401(6) Å) and Nd–Nd (4.1886(6) Å) in Ce_2AgGe_3, Pr_2AgGe_3 and Nd_2AgGe_3, respectively, which much larger than the expected bond distance of Ce–Ce (3.66 Å) [47], Pr–Pr (4.12 Å) [31] and Nd–Nd (4.06 Å) [35]. The shortest bond distance of M–M (M=Ag+Ge) in Ce_2AgGe_3, Pr_2AgGe_3 and Nd_2AgGe_3 are 2.4446(14) Å, 2.429(2) Å and 2.4211 (16) Å, respectively, very close to the calculated Ge–Ge bond distances of 2.44 Å [47], which suggests the germanium contribution at the 2*d* Wyckoff site but it is less than the atomic radii of Ag–Ag (2.88 Å) and Ge–Ag (2.85 Å) [47]. The shortest RE–M bond distances in Ce_2AgGe_3, Pr_2AgGe_3 and Nd_2AgGe_3 are 3.2508(7) Å, 3.2311(10) Å and 3.1996(5) Å, respectively. Selected bond lengths for Ce_2AgGe_3, Pr_2AgGe_3 and Nd_2AgGe_3 are listed in Table 4. The coordination environments of *RE* and M sites are shown in Fig. 3b and c, respectively. The rare earth atoms are coordinated by 12 M atoms forming a pseudo-Frank–Kasper cage. The M sites, on the other hand, form tricapped trigonal prism comprised of a total 9 metal atoms, 3M atoms and six RE atoms [M_3RE_6].

3.2. Magnetic properties

The temperature dependent magnetic measurements were carried out in an applied magnetic field of 100 Oe for Ce_2AgGe_3, Pr_2AgGe_3 and Nd_2AgGe_3 as shown in Figs. 4a, 5a and 6a, respectively. At higher temperature, Ce_2AgGe_3 and Pr_2AgGe_3 obeyed Curie–Weiss (CW) law but Nd_2AgGe_3 obeyed modified CW law i.e $\chi(T)=\chi+C/(T-\theta_p)$ where, χ_o accounts for the temperature independent part (TIP) of magnetic susceptibility. Upon cooling, the magnetic susceptibility curve of Ce_2AgGe_3 increases sharply below 15 K, which could arise due to ferromagnetic interaction. The CW fitting of the inverse magnetic susceptibility data in the range of 160–300 K yielded an effective magnetic moment of (μ_{eff}) 2.53 μ_B/Ce^{3+} and Curie paramagnetic temperature (θ_p) 7 K respectively. The magnetic moment value is very close to the spin only value of 2.54 μ_B/Ce^{3+} [23]. At lower applied magnetic field (10 Oe), the compound undergoes antiferromagnetic ordering at around 6.4 K (Fig. S1), which is suppressed to some extent at high field (100 Oe). A bifurcation of the zero-field cooled (ZFC) and field cooled (FC)

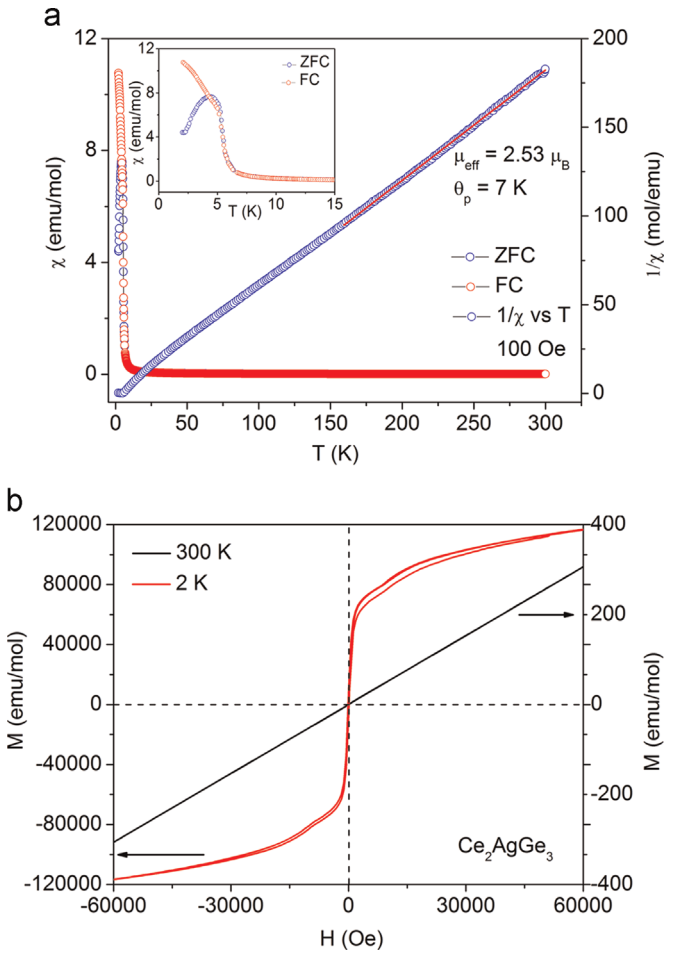

Fig. 4. (a) Temperature dependence of the molar magnetic susceptibility of Ce_2AgGe_3 at 100 Oe applied magnetic field plotted against the *X* axis on the left-hand side. Plot on the right-hand side shows the temperature dependence of the molar inverse magnetic susceptibility. The inset shows the magnetic susceptibility at FC and ZFC modes. (b) Magnetization measured as a function of magnetic field at $T=2$ K and 300 K.

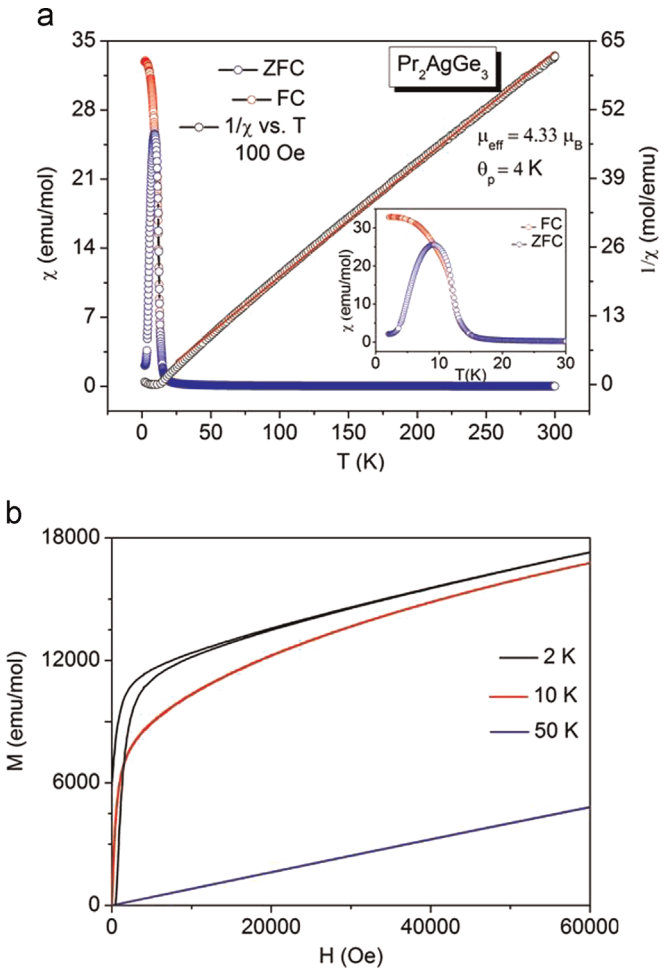

Fig. 5. (a) Magnetic susceptibility ($\chi=M/H$) as a function of temperature for Pr_2AgGe_3 (polycrystalline) samples measured in a dc field of 100 Oe. (b) Magnetization measured as a function of magnetic field at $T=2$ K, 10 K and 50 K.

susceptibility curves was observed which could arise due to various reasons like magnetic anisotropy and grain boundary pinning effects, etc (inset of Fig. 4) [48]. The field dependent magnetization study at 2 K shows that Ce_2AgGe_3 exhibits sharp rise in magnetization (M) for small change in field (H). Above few kOe, M varies non-linearly with H, and exhibits hysteresis $H\rightarrow 0$ as shown in Fig. 4b [48,49]. Such a behavior may arise due to spin-flop transition. Magnetization of cerium compound at room temperature varies linearly with H, which confirms that the sample is single-phase and there are no undesirable magnetic impurities.

In the case of Pr_2AgGe_3, the temperature dependent magnetic susceptibility curve increases rapidly around 15 K followed by a broad cusp and rapid falling of χ on further decrease in T down to 10 K, followed by a bifurcation in ZFC and FC curves (Fig. 5a) suggesting magnetic anisotropy or weak ferromagnet [50] like behavior. The effective magnetic moment (μ_{eff}) and curie paramagnetic temperature (θ_p) were calculated to be 4.33 μ_B/Pr^{3+} and 4 K, respectively using the CW fit of the inverse susceptibility curve in the temperature range of 25–300 K. The magnetic moment of the compound is slightly higher than the spin only value of Pr (3.58 μ_B/Pr^{3+}) [16] probably due to conduction electron polarization as observed in a similar compounds like Tb_2CuIn_3, Tb_2CuGe_3 and $EuAuIn_4$ [48,51] although it was not reported in Pr based compounds. The positive θ_p suggests that a ferromagnetic interaction exists among the adjacent spins, but very weak in nature. The field dependent magnetization curve of Pr_2AgGe_3 shows a weak hysteresis at 2 K indicating ferromagnetic transition (Fig. 5b). The temperature dependent M vs. H data shows that this weak ferromagnetic coupling is suppressed at higher temperatures (10 and 50 K).

The magnetic susceptibility of Nd_2AgGe_3 shows a large increase below 25 K and has two maxima at $T_{N1}=3.5$ K and $T_{N2}=11.8$ K (Fig. 6a) which are well supported by the temperature dependent resistivity data. The residual magnetic susceptibility (χ_0), effective magnetic moment (μ_{eff}) and Curie paramagnetic temperature (θ_p) for this compound are -0.0013 emu/mol, 3.47 μ_B/Nd (theoretical effective paramagnetic moment for Nd^{3+} is 3.62 μ_B) [52] and 12 K, respectively obtained from the fitting of inverse molar magnetic susceptibility with modified Curie–Weiss law. This kind of multiple magnetic transitions is not uncommon and was also observed in Nd_5Ge_3 [53,54]. The field dependent magnetization data at 2 and 300 K for Nd_2AgGe_3 have been plotted in Fig. 6b. M varies linearly with H in the measurement done at 300 K. At low temperature (2 K), a strong hysteresis is observed, which indicates ferrimagnetic like-coupling is the dominant magnetic interactions among the magnetic spins. It is not clear at this moment that what should be the reason for a ferrimagnetic like behavior, since there is only one Nd site per formula unit in this structure. However, owing to the fact that there are two antiferromagnetic transitions, it is possible that at low temperatures, both the antiferromagnetic states coexist, giving rise to such a hysteretic magnetization behavior. Ferrimagnetic like state, two magnetic transitions and

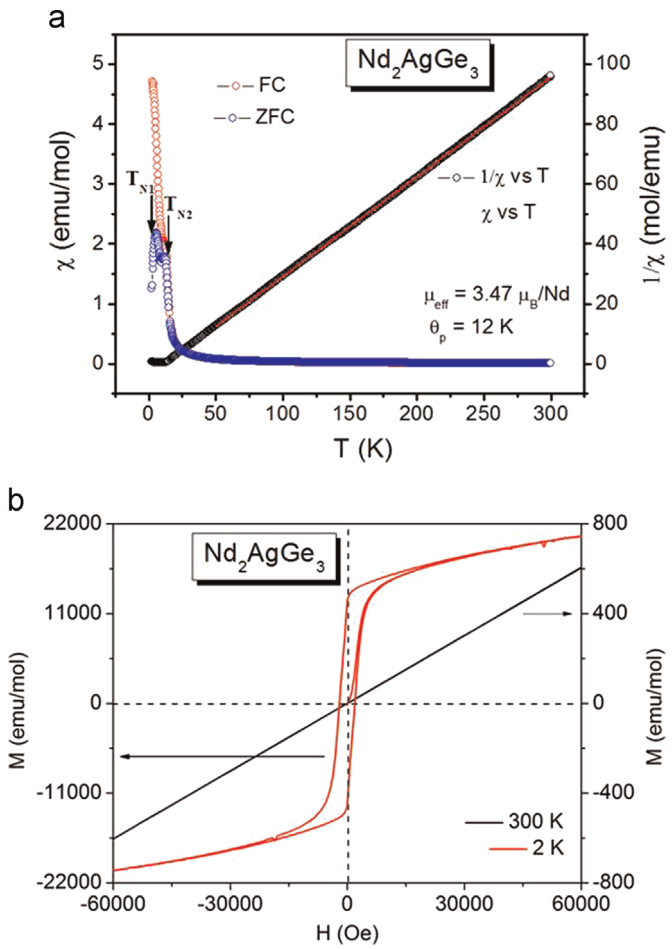

Fig. 6. (a) Magnetic susceptibility ($\chi = M/H$) as a function of temperature for Nd_2AgGe_3 (polycrystalline) samples measured in a dc field of 100 Oe. (b) Magnetization measured as a function of magnetic field at $T = 2$ K, and 300 K.

strong magnetic anisotropy makes this system an interesting candidate for detailed study using different probes and techniques.

3.3. Resistivity

The electrical resistivity of Ce_2AgGe_3, Pr_2AgGe_3 and Nd_2AgGe_3 are shown in Fig. 7. In the high temperature range, resistivity increases with increase in temperature for all the samples which is a typical and common behavior of metallic systems. The resistivity of Ce_2AgGe_3 (Fig. 7a) measured is equal to 10.86 μΩ cm at 200 K, decreases with temperature down to about 22 K [55] beyond which it increases up to 15 K. This behavior is reminiscent of Kondo scattering which has been observed in many other Ce based compounds like Ce_2RhSi_3 [23]. At low temperature region, ρ vs. T shows a maxima at 6.4 K and finally drops down to a value of 10.2 μΩ cm at 3 K indicating a magnetic phase transition in corroboration with the magnetic susceptibility data. The resistivity of Pr_2AgGe_3 (Fig. 7b) decreases linearly with decreasing temperature from 200 K down to 15 K followed by a maxima at 11 K indicating the magnetic ordering observed in magnetic susceptibility measurement. A similar behavior was also observed in case of Pr_2CuSi_3 [13]. Nd_2AgGe_3 also follows the same trend at higher temperature range wherein the resistivity decreases almost linearly down to 25 K. Below this temperature, a dip is observed around 20 K which is followed by a rise in resistivity with decrease in temperature (Fig. 7d). The occurrence of a dip in the low temperature resistivity plot in a Nd-based intermetallic compound is unusual since this phenomenon cannot be attributed to Kondo effect arising from Nd f-electrons. The situation is similar to that observed in cases of previously reported $GdPd_2Si$ [56] and $GdNi_2Si_2$ [57] where the authors have proposed spin-fluctuations at the transition metal lattices as the possible origin of increase in resistivity at low temperature. The actual reason for this phenomenon, however, still remains questionable and urges for further investigations.

4. Concluding remarks

We have thus synthesized already known Pr_2AgGe_3 and two new compounds namely, Ce_2AgGe_3 and Nd_2AgGe_3, which crystallize in the tetragonal α-$ThSi_2$ type structure. All the compounds reported here show interesting magnetic properties which provide a robust platform for further detailed study of the magnetic structure of these compounds using neutron diffraction technique. Existence of these compounds in the RE_2AgGe_3 series further motivated us to look for new compounds with other rare earth elements. Preliminary attempts to synthesize the Sm and Gd analogs by arc melting technique were unsuccessful; however, we are currently experimenting with different methods and various reaction conditions.

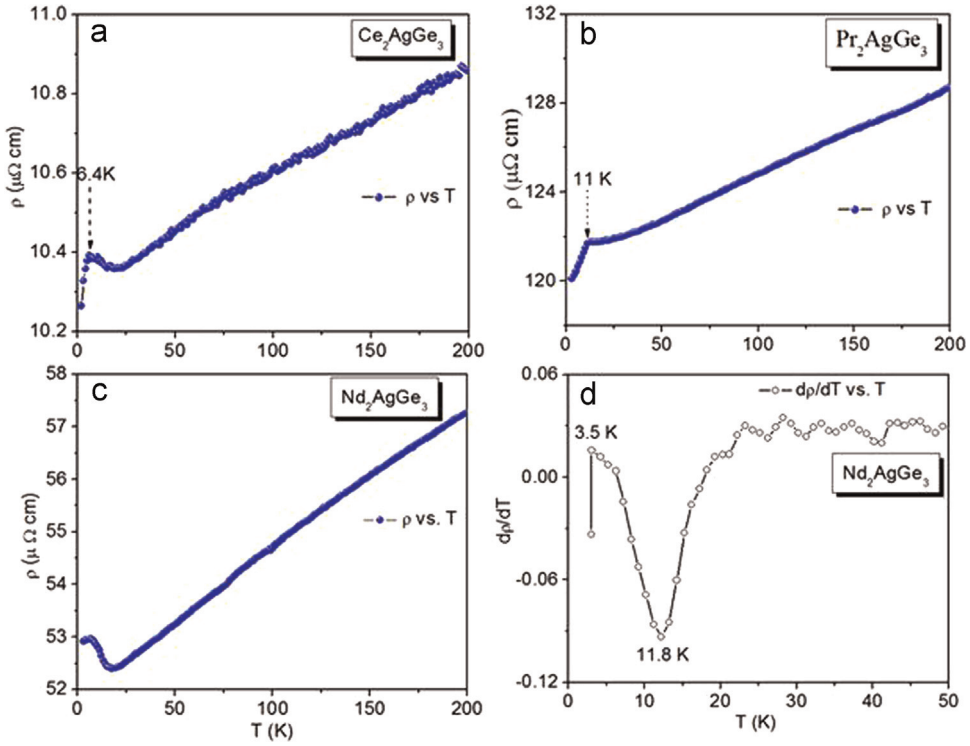

Fig. 7. Electrical resistivity (ρ) of (a) Ce_2AgGe_3, (b) Pr_2AgGe_3 and (c) Nd_2AgGe_3 measured as a function of temperature. (d) First order derivative of resistivity with respect to temperature for Nd_2AgGe_3.

Acknowledgments

We are grateful to Prof. C.N.R. Rao for his kind support. We thank JNCASR, UGC-DAE CSR (Project no. CRS-M-166), Sheikh Saqr Laboratory for the financial support. S.S. thanks CSIR, India for research fellowship. D.M., P.H. and D.K. thank the UGC-DAE CSR, Mumbai Center for project fellowship and S.C.P. thanks DST for Ramanujan fellowship (Grant SR/S2/RJN-24/2010).

Appendix A. Suplementary Information

Supplementary data associated with this article can be found in the online version at http://dx.doi.org/10.1016/j.jssc.2015.06.003.

References

[1] Z.-Y. Pan, C.-D. Cao, X.-J. Bai, R.-B. Song, J.-B. Zheng, L.-B. Duan, Chin. Phys. B 22 (2013) 056102.
[2] S.C. Peter, U. Subbarao, S. Sarkar, G. Vaitheeswaran, A. Svane, M.G. Kanatzidis, J. Alloy. Compd. 589 (2014) 405–411.
[3] S.R. Saha, H. Sugawara, T.D. Matsuda, Y. Aoki, H. Sato, E.V. Sampathkumaran, Phys. Rev. B: Condens. Matter 62 (2000) 425–429.
[4] A.P. Pikul, D.K. aczorowski, T. Plackowski, A. Czopnik, H. Michor, E. Bauer, G. Hilscher, P. Rogl, Y. Grin, Phys. Rev. B: Condens. Matter 67 (2003) 224417–224426.
[5] M. Frontzek, A. Kreyssig, M. Doerr, A. Schneidewind, J.U. Hoffmann, M. Loewenhaupt, J. Phys. Condens. Matter 19 (2007) 145276–145284.
[6] R. Feyerherm, A. Amato, C. Geibel, F.N. Gygax, P. Hellmann, R.H. Heffner, D. E. MacLaughlin, R. MullerReisener, Phys. Rev. B 56 (1997) 699–710.
[7] C.P. Sebastian, G. Heymann, B. Heying, U.C. Rodewald, H. Huppertz, R. Pöttgen, Z. Anorg. Allg. Chem. 633 (2007) 1551–1555.
[8] M. Frontzek, A. Kreyssig, M. Doerr, J.U. Hoffman, D. Hohlwein, H. Bitterlich, G. Behr, M. Loewenhaupt, Physica B 350 (2004) E187–E189.
[9] E.V. Sampathkumaran, I. Das, R. Rawat, S. Majumdar, Appl. Phys. Lett. 77 (2000) 418–420.
[10] S.C. Peter, M. Chondroudi, C.D. Malliakas, M. Balasubramanian, M. G. Kanatzidis, J. Am. Chem. Soc. 133 (2011) 13840–13843.
[11] B. Chevalier, E. Gaudin, A.F. Al Alama, S.F. Matara, F. Weilla, B. Heying, R. Pöttgen, Z. Naturforschung 63b (2008) 685–694.
[12] D.X. Huo, J. Sakurai, T. Kuwai, Y. Isikawa, Q.F. Lu, Phys. Rev. B 64 (2001) 224405.
[13] C. Tien, L. Luo, J.S. Hwang, Phys. Rev. B. 56 (1997) 11710.
[14] J.S. Hwang, K.J. Lin, C. Tien, Solid State Commun. 100 (1996) 169.
[15] D.X. Li, X. Zhao, S. Nimori, J. Phys.: Condens. Matter 21 (2009) 026006.
[16] J.W. Chen, S.Y. Guan, C.H. Wang. The 2nd International Symposium on Advanced Magnetic Materials and Applications, 266, 012006, July 12–16, 2010 Sendai, Japan (2011).
[17] D.P. Rojas, J.R. Fernández, J.I. Espeso, J.C. Gómez Sal, L.M. da Silva, F.G. Gandra, A.O. dos Santos, A.N. Medina, J. Magn. Magn. Mater. 322 (2010) 3192.
[18] R.A. Gordon, C.J. Warren, M.G. Alexander, F.J. Disalvo, R. Pöttgen, J. Alloy. Compd. 24 (1997) 248.
[19] A. Szytuła, M. Hofmann, B. Penc, M. Slaski, S. Majumdar, E. V. Sampathkumaran, A. Zygmunte, J. Magn. Magn. Mater. 202 (1999) 365.
[20] M. Szlawska, D. Kaczorowski, Phys. Rev. B. 84 (2011) 094430.
[21] K. Yubuta, T. Yamamura, Y. Shiokawa, J. Phys.: Condens. Matter 18 (2006) 6109.
[22] D.X. Li, S. Nimori, Y. Shiokawa, Y. Haga, E. Yamamoto, Y. Onuki, Solid State Commun. 120 (2001) 227.
[23] N. Kase, T. Muranaka, J. Akimitsu, J. Magn. Magn. Mater. 321 (2009) 3380.
[24] T. Cheng, H.F. Chung, S.W. Ching, J.L. Jenq, Phys. Rev. B 61 (2000) 12151–12158.
[25] V. Raghavan, J. Ph. Equilib. Diffus. 29 (2008) 436–437.
[26] P.S. Salamakha, M.B. Konyk, R.B. Dzyanyi, O.L. Sologub, O.I. Bodak, Pol. J. Chem. 70 (1996) 270–274.
[27] A.V. Morozkin, J. Alloy. Compd. 370 (2004) L1–L3.
[28] D. Kalsi, S. Udumula, S. Rayaprol, S.C. Peter, J. Solid State Chem. 212 (2014) 73–80.
[29] I. Mayer, I. Felner, J. Solid State Chem. 8 (1973) 355–356.
[30] M.F. Fedyna, V.K. Pecharskii, O.I. Bodak. Dopov. Akad. Nauk Ukr. RSR B, 1987, 2–50.
[31] M.M. Dzioba, I.A. Savysyuk, O.O. Shcherban, E.I. Gladyshevskii. Visn. L'viv. Derzh. Univ. (Ser. Khim.),1996, 36-59.
[32] M.F. Fedyna, O.I. Bodak, V.K. Pecharskii, Inorg. Mater. 27 (1991) 918–920.
[33] P.Y. Demchenko, O.I. Bodak, J. Alloy. Compd. 307 (2000) 215–217.
[34] P.S. Salamakha, P.Y. Demchenko, O.L. Sologub, O.I. Bodak, J. Alloy. Compd. 278 (1998) 227–230.
[35] O.I. Bodak, P.S. Salamakha, O.L. Sologub, J. Alloy. Compd. 256 (1997) L8–L9.
[36] C.P. Sebastian, C.D. Malliakas, M. Chondroudi, I. Schellenberg, S. Rayaprol, R. D. Hoffmann, R. Pöttgen, M.G. Kanatzidis, Inorg. Chem. 49 (2010) 9574–9580.
[37] S. Sarkar, M.J. Gutmann, S.C. Peter, CrystEngComm 15 (2013) 8006–8013.
[38] S. Sarkar, S.C. Peter, J. Chem. Sci. 124 (2012) 1385–1390.
[39] F. Merlo, M. Pani, F. Canepa, M.L. Fornasini, J. Alloy. Compd. 264 (1998) 82–88.
[40] M. Pani, F. Merlo, M.L. Fornasini, Z. Kristallogr. 214 (1999) 108–110.
[41] R. Pöttgen, B. Gibson, R.K. Kremer, Z. Kristallogr. 212 (1997), p.58.
[42] C.P. Sebastian, M.G. Kanatzidis, J. Solid State Chem. 183 (2010) 878–882.
[43] S. Sarkar, D. Kalsi, S. Rayaprol, S.C. Peter, J. Alloy. Compd 632 (2015) 172–177.
[44] G.M. Sheldrick, SHELXTL 5.10; Bruker Analytical X-ray Systems, Bruker AXS Inc., Madison, WI, 1998.

[45] G.M. Sheldrick, SHELXTL, Structure Determination Program (Version 5), Siemens Analytical X-ray Instruments, Bruker AXS Inc., Madison, WI, 1995.
[46] H. Putz, K.i.G.B. BrandenburgGb R, (Ed.), CRYSTAL IMPACT, pp. 53227.
[47] L. Pauling. The Nature of the Chemical Bond, Third ed, 1960, Cornel University Press, Ithaca, NY.
[48] S. Majumdar, E.V. Sampathkumaran, Solid State Commun. 117 (2001) 645–648.
[49] S. Sarkar, U. Subbarao, B. Joseph, S.C. Peter, J. Solid State Chem. 225 (2015) 181–186.
[50] A. Lacerda, P.C. Canfield, W.P. Beyermann, M.F. Hundley, J.D. Thompson, G. Sparn, Z. Fisk, C. Burns, D. Barnhart, A.D. Lawson, G.H. Kwei, J. Goldstone, J. Alloy. Compd. 181 (1992) 191.
[51] S. Sarkar, M.J. Gutmann, S.C. Peter, Dalton Trans. 43 (2014) 15879–15886.
[52] R. Kozak, D. Kaczorowski, R. Gladyshevskii, Chem. Met. Alloy. 5 (2012) 16–22.
[53] S.B. Roy, J.K. Chattopadhyay, P. Chaddah, J.D. Moore, G.K. Perkins, L.F. Cohen, K. A. GschneidnerJr, V.K. Pecharsky, Phys. Rev. B 74 (2006) 012403.
[54] T. Tsutaoka, A. Tanaka, Y. Narumi, M. Iwaki, K. Kindo, Physica B. 405 (2010) 180–185.
[55] R.V. Dremov, N. Koblyuk, Y. Mudryk, L. Romaka, V. Sechovsky, J. Alloy. Compd. 317 (2001) 293–296.
[56] R. Rawat, I. Das, J. Phys. Condens. Matter. 13 (2001) L57.
[57] I. Das, E.V. Sampathkumaran, Phys. Rev. B 49 (1994) 3972–3974.